Shadow camera system for the validation of nowcasted plant-size irradiance maps

Pascal Kuhn, pascal.kuhn@dlr.de

S. Wilbert, C. Prahl, D. Schüler, T. Haase, T. Hirsch, M. Wittmann, L. Ramirez, L. Zarzalejo, A. Meyer, L. Vuilleumier, P. Blanc, R. Pitz-Paal

European Conference for Applied Meteorology and Climatology 2017, 6-Sept-2017

DLR Deutsches Zentrum für Luft- und Raumfahrt
German Aerospace Center

GOBIERNO DE ESPAÑA
MINISTERIO DE CIENCIA E INNOVACIÓN

Ciemat
Centro de Investigaciones Energéticas, Medioambientales y Tecnológicas

MeteoSwiss

MINES ParisTech

Overview

1. Importance of reference irradiance maps for nowcasting systems
2. Approach & methodology of the shadow camera system
3. Validation of the shadow camera system
4. Conclusion and further work

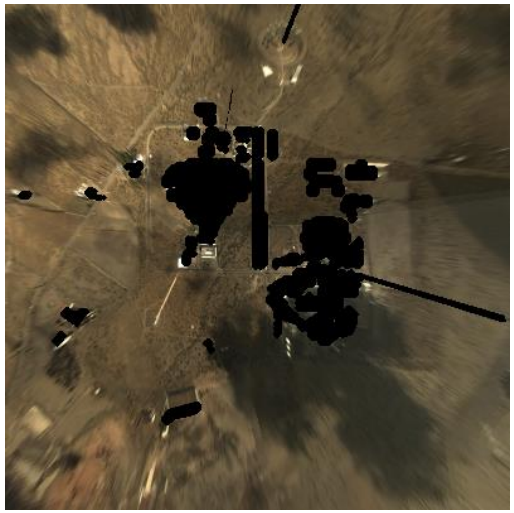

Validation of all-sky imager based nowcasting systems

All-sky imager based nowcasting systems support plant & grid operations

- Ramp rates regulations for solar plants are discussed
- Ramp rate penalties can reduce gross revenue of solar plants by 20% [1]
- All-sky imager based nowcasting system like the WobaS system [2] are one solution for this challenge

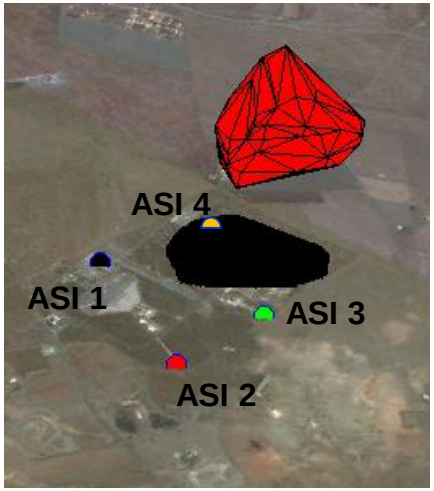

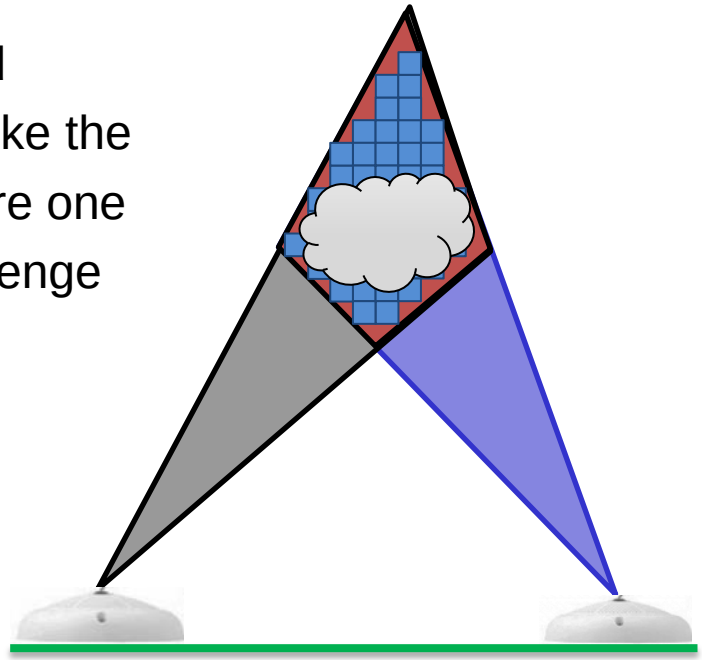

ASI 1 of 4 ASI 2 of 4

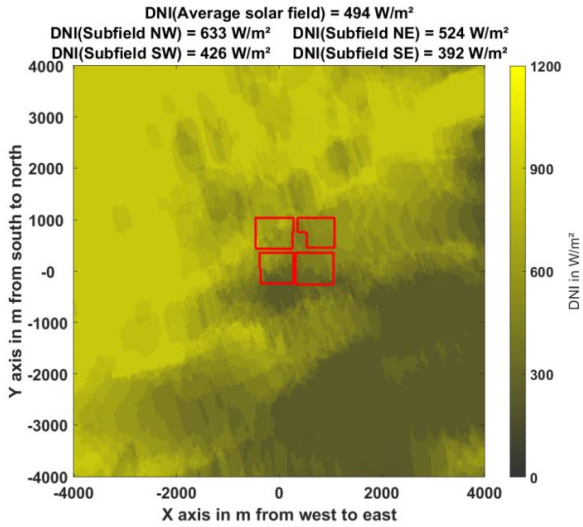

[1] D. Cormode, A. Lorenzo, W. Holmgren, S. Chen and A. Cronin, "The economic value of forecasts for optimal curtailment strategies to comply with ramp rate rules," *2014 IEEE 40th Photovoltaic Specialist Conference (PVSC)*, Denver, CO, 2014, pp. 2070-2075. doi: 10.1109/PVSC.2014.6925334

[2] Kuhn, P., et al., "Validation of an All Sky Imager based nowcasting system for industrial PV plants", EUPVSEC 2017, submitted to Progress in Photovoltaics.

DLR

Validation of all-sky imager based nowcasting systems

Spatial and temporal aggregation effects must be considered

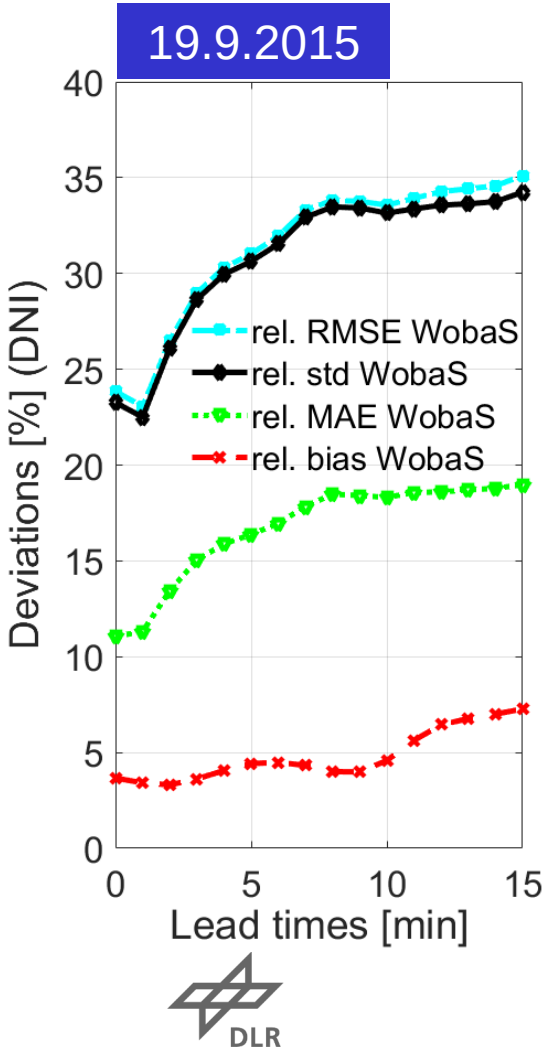

Nowcasting systems are usually validated against radiometers e.g. for one-minute averages.

CSP plants have thermal inertia of several minutes, which is not considered this way (similar: PV + battery).

Temporal aggregation effects change the behavior.

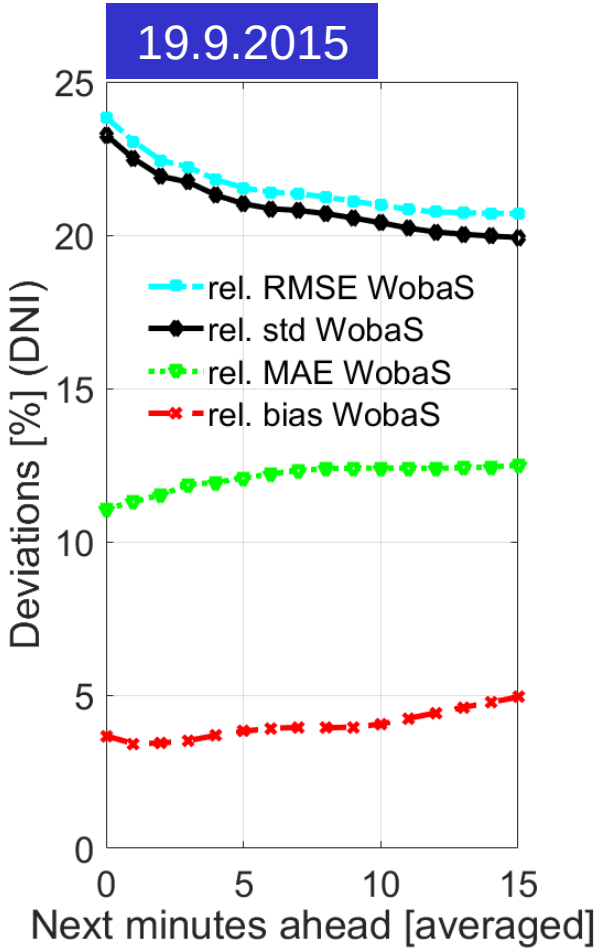

What about spatial aggregation?

DLR

Generation of reference irradiance maps

Two options are available for highly spatially resolved irradiance maps

Grid of irradiance sensors [3]

- Straight forward approach
- Costly and labor intensive
- Limited spatial coverage

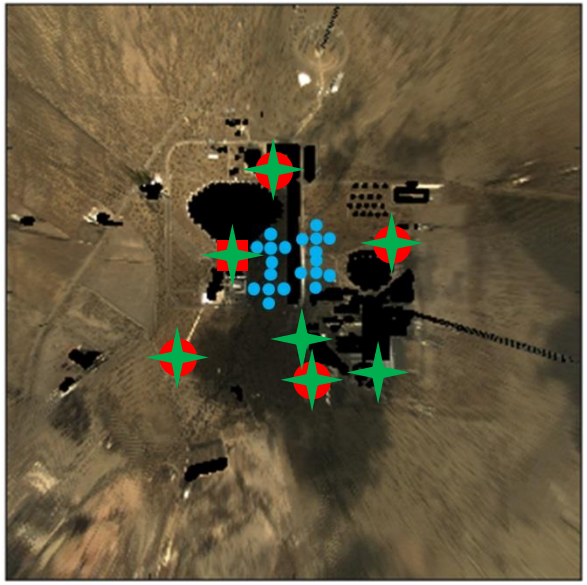

- 4 all-sky imager
- 6 shadow cameras
- 20 Si-pyranometers
- Pyrheliometers + pyranometers

Shadow camera system [4]

- Fairly inexpensive
- Low maintenance
- Large imaged area

[3] H. Schenk, et al., Design and Operation of an Irradiance Measurement Network, Energy Procedia, Volume 69, 2015, Pages 2019-2030, ISSN 1876-6102, http://dx.doi.org/10.1016/j.egypro.2015.03.212.(http://www.sciencedirect.com/science/article/pii/S1876610215005184)

[4] Kuhn, P., et al., “Shadow camera system for the generation of solar irradiance maps“, Solar Energy (2017), https://doi.org/10.1016/j.solener.2017.05.074.

Working principle of the shadow camera system

Six cameras provide raw images from which an orthoimage is derived

Six cameras

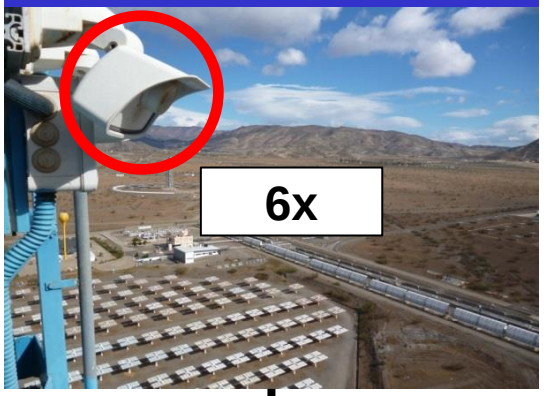

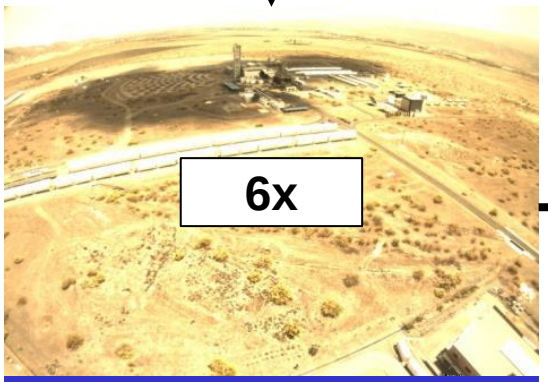

Six raw images

Orthoimage every 15 sec / 5m*5m

DLR

Working principle of the shadow camera system

Sunny and shaded reference orthoimages allow shadow detection

Sunny reference orthoimage

The current orthoimage is compared to sunny and shaded reference orthoimages for similar solar position

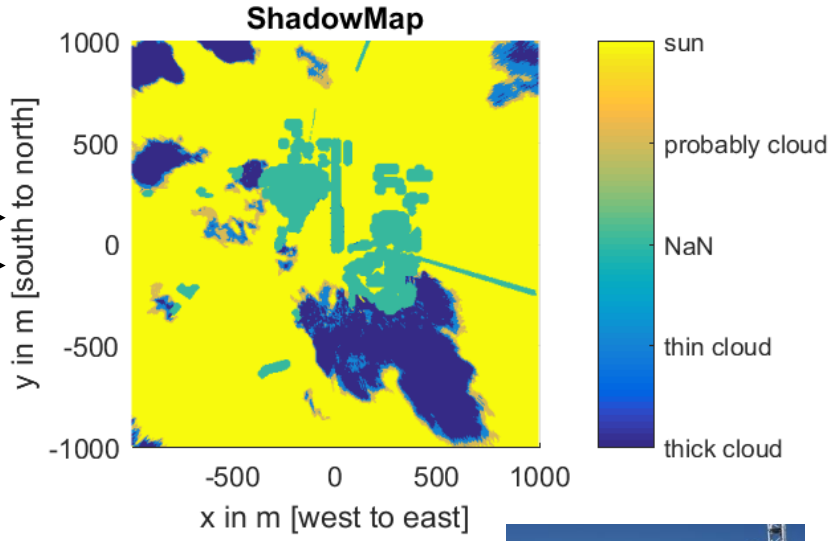

How do we obtain reference irradiance maps?

- For the unshaded areas: Clear Sky irradiance ⟷
- For the shaded areas:

why?

$$\textbf{(1)}\ DNI_{mn,current} = \frac{E_{BB,mn,current} - E_{BB,mn,shaded} \cdot \frac{DHI_{mn,current}}{DHI_{mn,shaded}}}{E_{BB,mn,sunny} - E_{BB,mn,shaded} \cdot \frac{DHI_{mn,sunny}}{DHI_{mn,shaded}}} \cdot DNI_{mn,sunny}$$

DLR

Working principle of the shadow camera system

Every pixel on the camera chip measures a broadband irradiance

Every pixel *m,n* images an area illuminated by DNI and DHI irradiance:

(2)

$$E_{BB,mn} = \alpha_{mn}\left(DNI_{mn} \cdot BRDF_{DNI,mn} + \sum_{i=1}^{N} DHI_{mn,i} \cdot BRDF_{DHI,mn,i}\right)$$

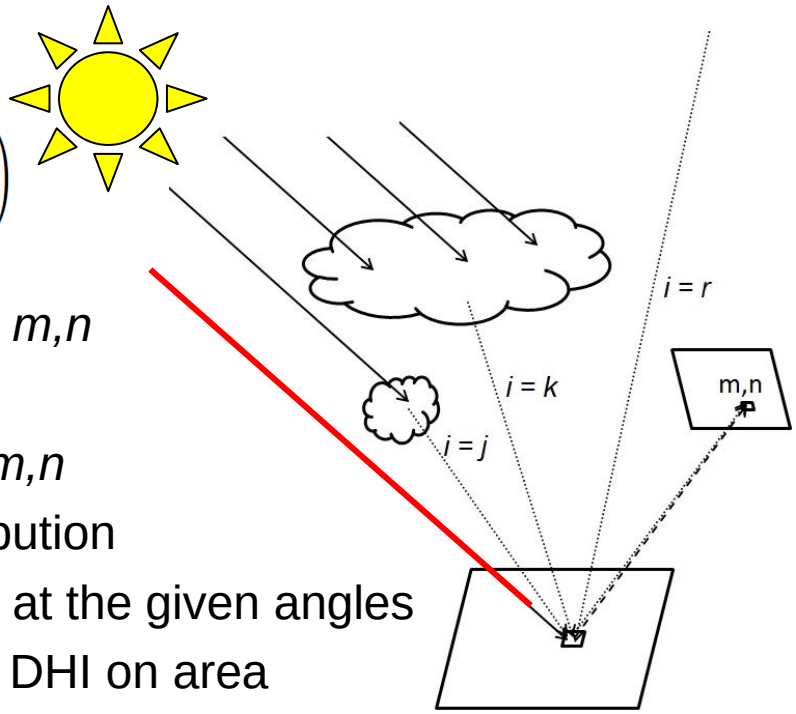

- $E_{BB,mm}$ broadband irradiance on pixel *m,n*
- α_{mn} pixel-wise calibration factor
- DNI_{mn} DNI on area imaged by pixel *m,n*
- $BRDF_{DNI,mn}$ bidirectional reflectance distribution function for pixel *m,n* and DNI at the given angles
- $DHI_{mn,i}$ irradiance contribution to total DHI on area imaged by pixel *m,n* from sky element *i* of *N*
- $BRDF_{DHI,mn,i}$ BRDF for $DHI_{mn,i}$

DLR

Working principle of the shadow camera system

A simplified BRDF and reference orthoimages lead to DNI formula

Further needed assumptions:

- DNI_{mn} for the shaded reference orthoimage is zero
- The relative angular diffuse radiance distribution of the sky is the same for all three orthoimages
- BRDFs for DNI are the same for all three orthoimages
- BRDFs for DHI are the same for all three orthoimages

This leads to

$$DNI_{mn,current} = \frac{E_{BB,mn,current} - E_{BB,mn,shaded} \cdot \frac{DHI_{mn,current}}{DHI_{mn,shaded}}}{E_{BB,mn,sunny} - E_{BB,mn,shaded} \cdot \frac{DHI_{mn,sunny}}{DHI_{mn,shaded}}} \cdot DNI_{mn,sunny}$$

As we do not have pixel-wise DHI measurements, we furthermore assume that the DHI is constant over the imaged area.

DLR

Results: Accuracy of the shadow camera system

Looking at an example day

19.9.2015

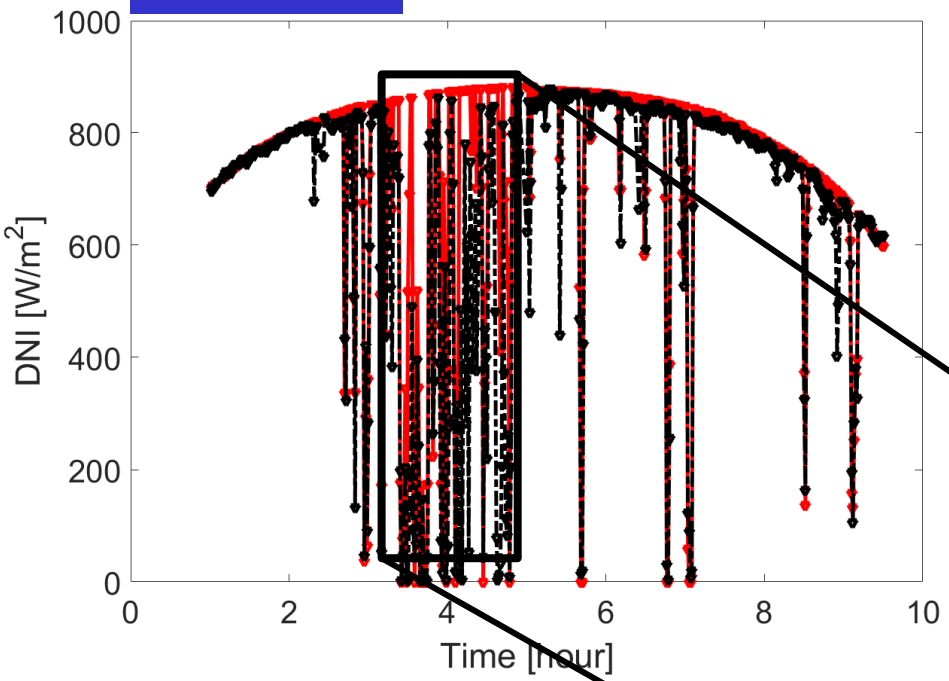

19.9.15	GHI	DNI
RMSE	48.8 W/m² (8.2%)	68.7 W/m² (10.0%)
MAE	37.0 W/m² (6.2%)	38.8 W/m² (5.7%)

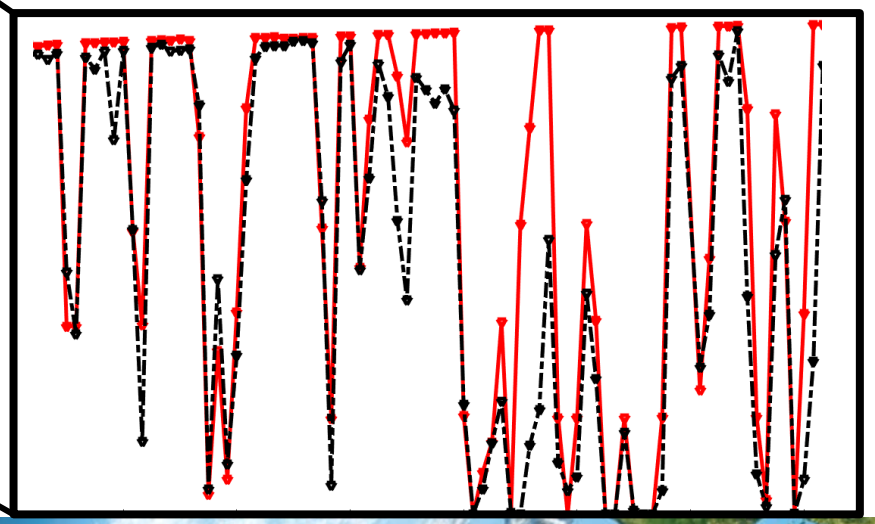

Spatial aggregation effects
Preliminary validation period of 5 days

- The validation of GHI reference maps is conducted with 23 pyranometers as reference for 23 pixels of the GHI map

- "Average of stations' GHI RMSE" is calculated as the mean of the RMSEs derived for all 23 pixels independently

- Spatial average is the RMSE of the average GHI of all 23 pixels for each timestamp

Validation period	average of stations' GHI RMSEs [W/m²]	23 pixel spatial average GHI RMSE [W/m²]
2015-09-18	35.2	30.7
2015-09-19	62.1	48.8
2016-05-11	98.0	89.8
2016-09-01	46.8	39.9
2016-12-09	40.1	43.7

Spatial aggregation effects are visible even for averages of only 23 pyranometers

DLR

WobaS system compared to reference irradiance maps

For validations, spatial aggregation effects must be considered

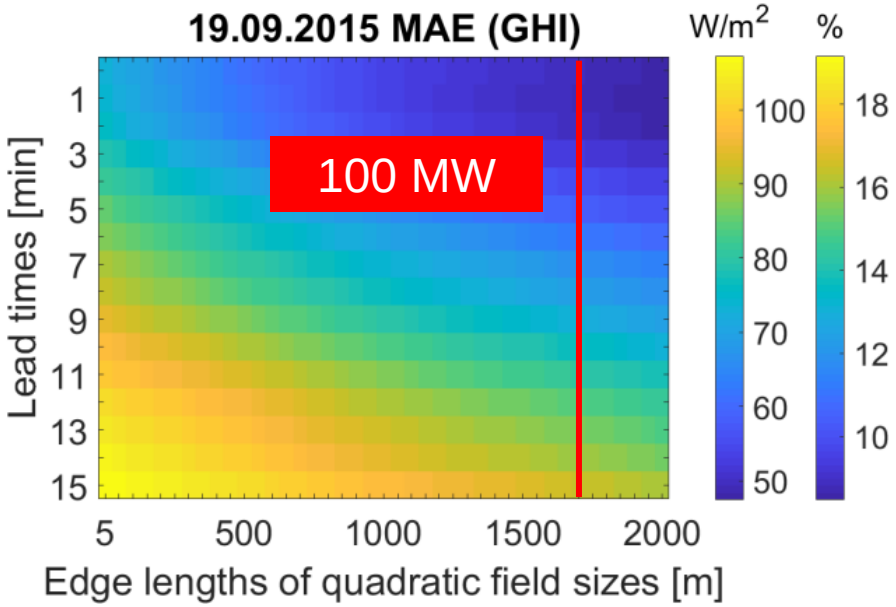

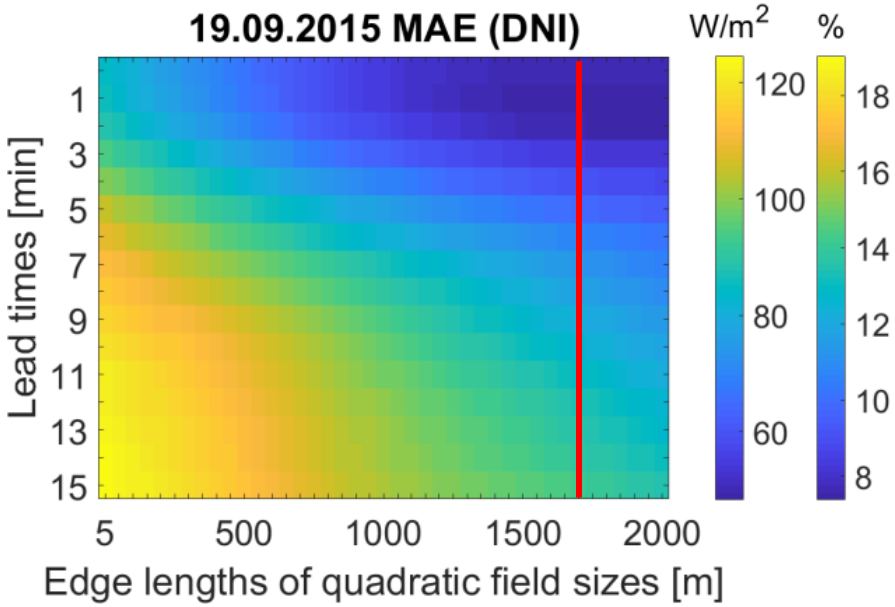

- Spatial aggregation significantly reduces deviations
- Spatial aggregation effects are inherent in industrial solar power plants
- Benchmarking of nowcasting systems must consider temporal and spatial aggregation effects

DLR

Conclusion and further work

- A shadow camera system is operated at PSA since 2015
- Reference DNI, GHI and GTI irradiance maps are available in high spatial (5m*5m) and temporal (15s) resolutions
- The shadow camera system was used for the validation of all-sky imager based nowcasting systems
- Cloud motion vectors can be derived and used as reference for ground based sensors, satellite based products and NWP models
- Future work:
  - Validation of a shadow camera based nowcasting system

DNICast

WobaS

Supported by:

Federal Ministry for Economic Affairs and Energy

on the basis of a decision by the German Bundestag

PreFlexMS
PREDICTABLE&FLEXIBLE SOLAR POWER WITH MOLTEN SALT ENERGY STORAGE

Thank you! **Questions?**

Thank you!

Questions?

Pascal.Kuhn@dlr.de

DLR

Publications

- Kuhn, P., et al., “Shadow camera system for the generation of solar irradiance maps“, Solar Energy (2017), https://doi.org/10.1016/j.solener.2017.05.074.
- Kuhn, P., et al., “Validation of an All Sky Imager based nowcasting system for industrial PV plants”, EUPVSEC 2017, submitted to Progress in Photovoltaics.
- Kuhn, P., et al., “Benchmarking three low-cost, low-maintenance cloud height measurement systems and ECMWF cloud heights”, submitted to Solar Energy (2017).
- Kuhn, P., et al., “Field validation and benchmarking of a cloud shadow speed sensor”, submitted to Solar Energy (2017).
- Kuhn, P., et al., “All-sky imager based ramp rate prediction for PV”, article of the month June 2017, Sun&Wind Energy, available online: http://www.sunwindenergy.com/content/sky-imager-based-ramp-rate-prediction-pv
- Kuhn, P.; Wilbert, S.; Prahl, C.; Kazantzidis, A.; Ramirez, L.; Zarzalejo, L.; Vuilleumier, L.; Blanc, P.; Pitz-Paal, R.; *Validation of nowcasted spatial DNI maps*, DNIcast Deliverable 4.1, available online: http://www.dnicast-project.net/.
- Kuhn, P., et al. „Validation of Spatially Resolved All Sky Imager Derived DNI Nowcasts”, AIP Conference Proceedings, 2017, http://aip.scitation.org/doi/abs/10.1063/1.4984522.
- See also: http://www.dlr.de/sf/en/desktopdefault.aspx/tabid-10436/20662_read-48274/

DLR

Further applications of shadow camera systems

Shadow camera systems can measure cloud motion vectors

Shadow camera

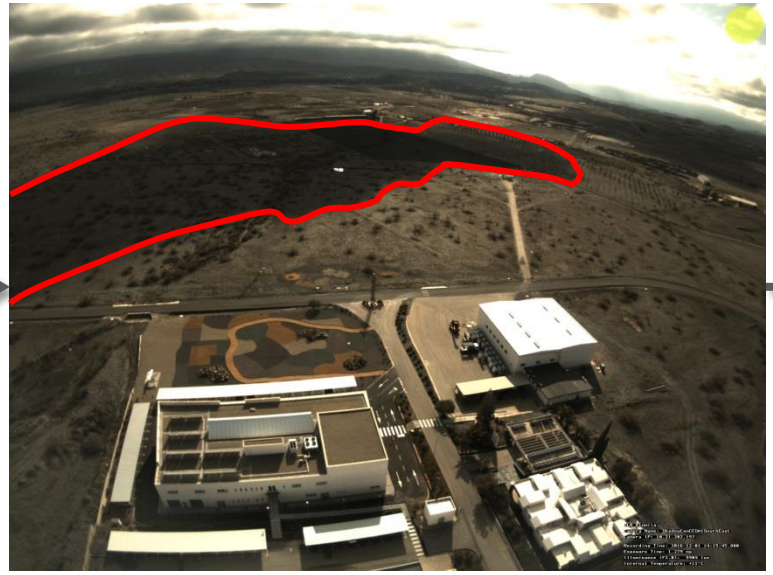

Shadow camera image (4 per minute)

Orthoimage (5m per pixel)

Velocities are measured without detecting shadows

Differential approach derives cloud motion vectors

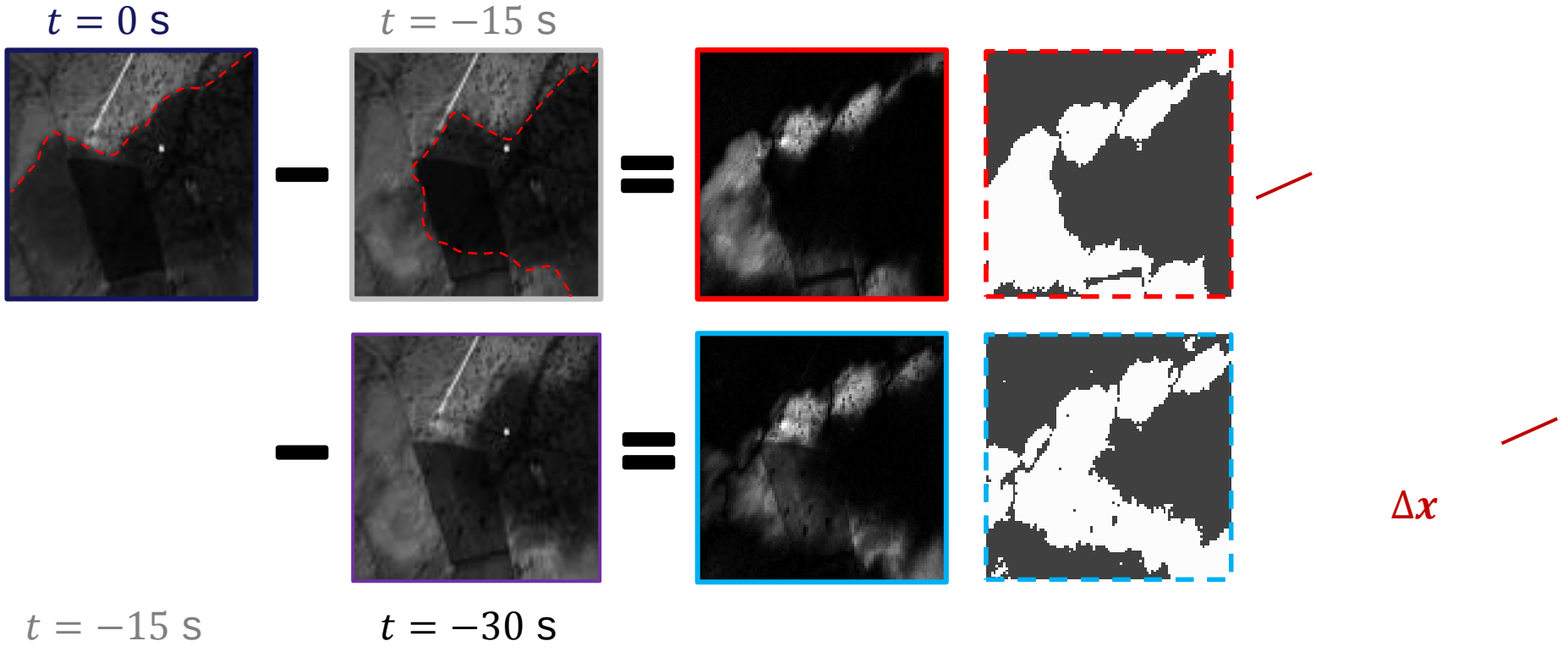

Shadow speed = $v_{m/s} = \frac{\Delta x \times k}{\Delta t}$

Δx: displacement [pixel]

k: meter/pixel

Δt: 15 s

DLR

Shadow cameras provide reference cloud velocities

Reference cloud shadow speed measurements are used for validations

- Shadow cameras provide reference cloud shadow motion vectors
- This data was used to validate the cloud shadow speed sensor [2], both for velocity and measured direction on 59 days
- Cloud motion vectors of NWP or satellite forecasts could potentially be validated on extensive periods

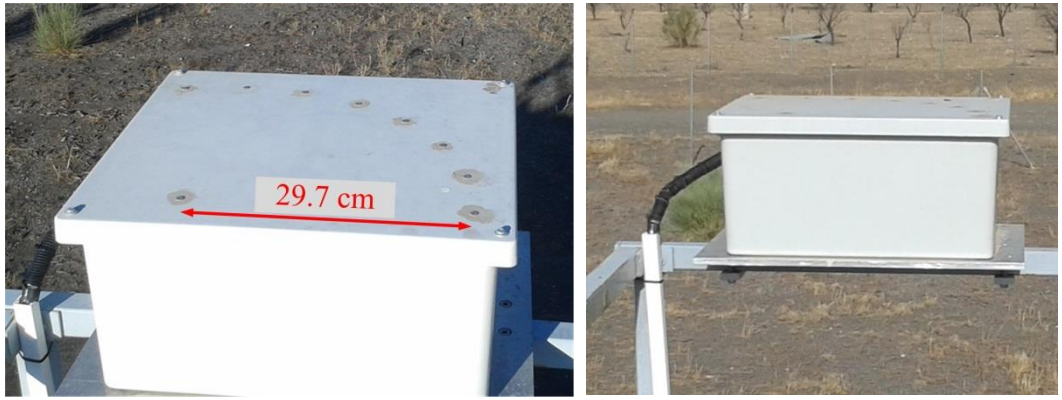

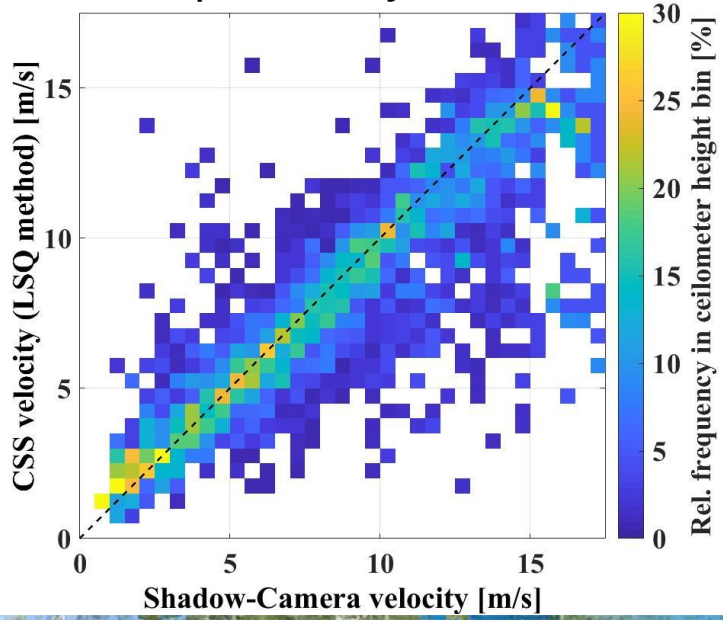

[2] Fung, Victor, et al. "Cloud speed sensor." *Atmospheric Measurement Techniques Discussions* 6.5 (2013). Doi: 10.5194/amtd-6-9037-2013

DLR

Shadow cameras can act as nowcasting systems

Shadow cameras have distinct advantages over all-sky imagers

Case study for Andasol plants:

- 2 cameras 20 km away 2 km above the plant on a mountain
- 10 km field of view around the plant
- Mean shadow velocity: 7.36 m/s

→ mean forecast horizon: 22.6 minutes